Angewandte Chemie
Eine Zeitschrift der Gesellschaft Deutscher Chemiker

Supporting Information

Single-Nanoparticle Collision Events: Tunneling Electron Transfer on a Titanium Dioxide Passivated n-Silicon Electrode

*Hyun S. Ahn and Allen J. Bard**

anie_201506963_sm_miscellaneous_information.pdf

Supporting Information

Experimental

General. All solutions were prepared using a Milli-Q deionized water. Anhydrous potassium phosphate monobasic (99% Fisher), anhydrous potassium phosphate dibasic (99% Fisher), 1,1'-ferrocenedimethanol (98%, Acros), titanium trichloride (12 % Ti in HCl solution, Sigma-Aldrich), anhydrous sodium sulfite (99%, Fisher), and potassium ferricyanide (99.95%, Fisher) were used as received. Arsenic-doped n-type (100) silicon wafer (0.001 – 0.005 Ω·cm) was obtained from EL-CAT Inc. and ohmic contact was provided by Ti/Au deposition on one side of the wafer. Standard RCA cleaning of the n-Si surface was performed before use. A 3M Kapton tape was used for masking out the electrode area on n-Si (see electrode preparation section below). A Harris micro punch (Electron Microscopy Science) of 0.5 mm diameter was used to generate electrode holes on the masking tape (see electrode preparation section below). Platinum nanoparticles used in collision experiments were obtained from nanoComposix (San Diego, CA). Nanoparticle size was 50 ± 5 nm (size distribution determined by NanoSight shown below). For all electrochemical measurements a Ag/AgCl reference electrode and a platinum wire counter electrode were used. All electrochemical measurements were conducted using a CH Instruments (Austin, TX) model 900b potentiostat. A Xe lamp (XBO 150 W, Osram, Germany) was used for illumination. A silicon photodetector (818-UV, Newport, Irvine, CA) with an attenuator (OD3, Newport) and an optical power meter (1830-C, Newport) were used to calibrate the light intensity. Scanning electron microscopy was conducted on a Quanta 650 FEG (FEI Company, Inc., Hillsboro, OR). Nanoparticle tracking analysis was performed on a NS500 NanoSight instrument (Malvern Ins. Co., Worcestershire, UK). Optical profilometry was performed on a WYKO NT9100 profiler (Veeco Instruments, Plainview, NY). Atomic force microscopy was performed on a Park Scientific AutoProbe scanning probe microscope in contact mode.

Photoelectrochemistry. The active areas of all electrodes used were defined by a masking tape (see below for details), rendering a circular area of *ca.* 600 μm diameter. A standard glass cell with a window to attach the working electrode was used. Front illumination of the sample was performed for photoelectrochemistry, with the light intensity of 100 $mW \cdot cm^{-2}$ at 500 nm wavelength. Chopped light LSV experiments were performed at a scan rate of 10 mV/s and light chopping in 5 s intervals.

Electrodeposition of *a*-TiO_2. The electrodeposition of *a*-TiO_2 was performed as described in the literature with moderate modifications.[1,2] $TiCl_3$ solution for the electrodeposition was prepared by diluting 12% $TiCl_3$ solution in HCl 1:20 in deionized water, followed by neutralization of the pH of the solution to 2.33 ± 0.03 by slow addition of 0.5 M $NaHCO_3$ solution. The pH adjustment was accompanied by color change of the solution from reddish purple to deep purple, and the added volume of the solution led to a final Ti^{3+} concentration of *ca.* 15 mM. The electrodeposition process was performed by applying – 0.01 V vs SCE under Xe lamp illumination. Deposition progress was monitored by chronoamperometry. Deposition time of 9 s was employed. The electrodes were dried thoroughly under flowing air following depositions to ensure full condensation of the deposited TiO_2. After two deposition cycles (9 s each), current due to photo-oxidation of FcDM was subdued as displayed in Figure 3a. Further deposition cycles to fully passivate the n-Si were not performed in order to ensure thin enough *a*-TiO_2 for tunneling electron transfer. The remaining uncovered electrode area (most likely in the form of pin-holes) were allowed to self-passivate by SiO_2 growth in an oxygen-saturated water for 72 h prior to use.[3]

Silicon Electrode Preparation

Silicon wafer, n-type (100), was cut into pieces of size *ca.* 2 cm x 2cm. An n-Si piece was then cleaned thoroughly for 2 – 5 minutes with 48 vol% HF to remove native oxide layer followed by several washes with deionized water. Cleaned n-Si piece was then covered by an electrically insulating masking tape (Kapton by 3M, thickness 55 µm measured by Wyko profilometer) with a d = 600 µm hole, which defined the exposed area as the working electrode for experiments (Figure S1). The consistency of the size of the hole in the masking tape was verified by CV of the defined electrodes as shown in Figure S1. On average, d = 600 µm electrode was obtained with less than 10 % variation in size.

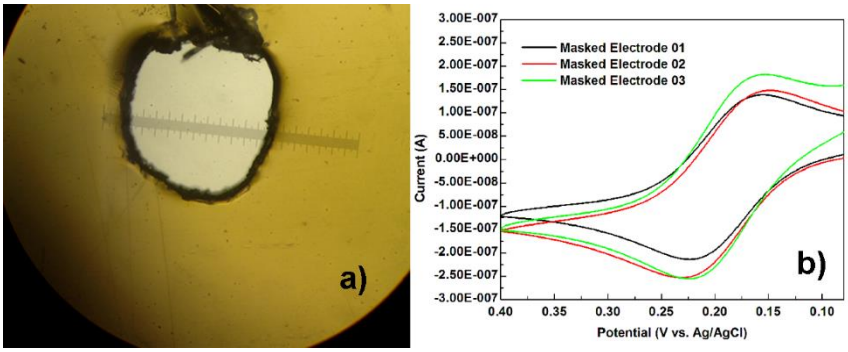

Figure S1. **a)** Microscope image of the masked electrode. **b)** Cyclic voltammograms obtained from three different masked Pt electrodes (1 mM FcDM, scan rate = 50 mV/s). Consistent masked area achieved each time with less than 10 % deviation. Average electrode diameter was 600 µm.

Thickness estimation of the amorphous TiO_2 layer

Attempts to best estimate the thickness of the electrodeposited amorphous TiO_2 film were made by atomic force microscopy (AFM) and optical profilometry. In our previous work, we have estimated the TiO_2 film thickness on a conducting surface by capacitance measurements (*ca.* 1 nm).[4] Here we have taken a freshly made sample of TiO_2 film on n-Si and analyzed it by AFM. In Figure S2 we see a region of different heights by *ca.* 1 nm in the AFM line scans, suggesting that the thickness of the amorphous TiO_2 layer can be estimated as *ca.* 1 nm. The AFM image was taken within 1 h of HF removal of the native SiO_2, and thus the low height region is surmised to be the bare n-Si surface. Optical profilometry (Figure S3) suggested a similar thickness for the TiO_2 film. We have found several cracks and ridges on the film ranging in thicknesses of 1 to 4 nm (see Figure S3 for examples). Optically visible cracks and ridges with heights in the order of 1 to 4 nm suggests that the thickness of our TiO_2 film is also in that height range. Direct tunneling electron transfer through parts of the film that is thin enough (~ 1 nm) is likely based on the AFM and profilometry observations.

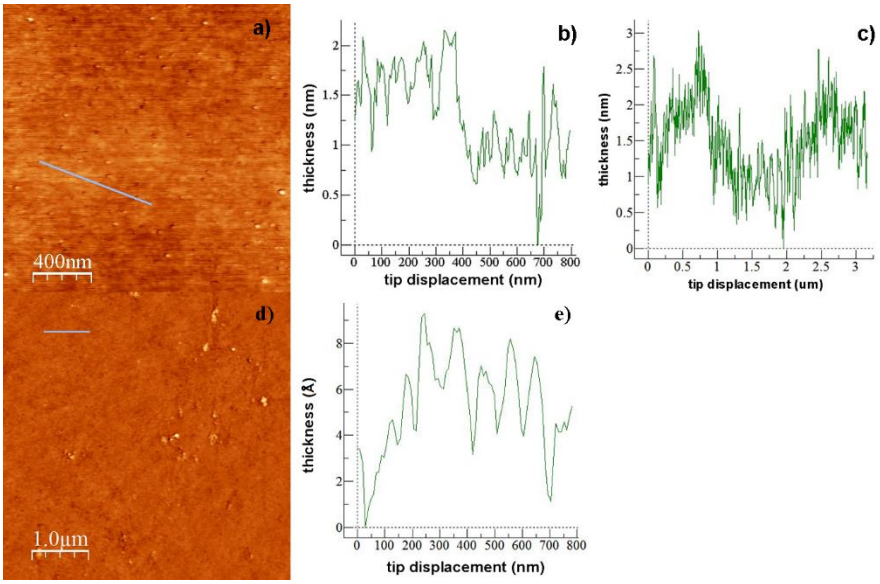

Figure S2. **a)** AFM topology of amorphous TiO_2 on n-Si, **b)** a line scan thickness profile showing the TiO_2 surface roughness and what seems to be a *ca.* 1 nm edge, **c)** another line scan thickness profile showing two regions of different height by *ca.* 1 nm. The lower region seems to be the bare n-Si surface, and the higher regions surrounding it is likely to be where the TiO_2 deposited. The sample was analyzed within 1 h of HF wash of the native SiO_2. **d)** AFM topology of bare n-Si, and **e)** showing a line scan of an n-Si surface. The bare n-Si displayed a much smoother image by AFM, and the line scan also showed roughness of several Å.

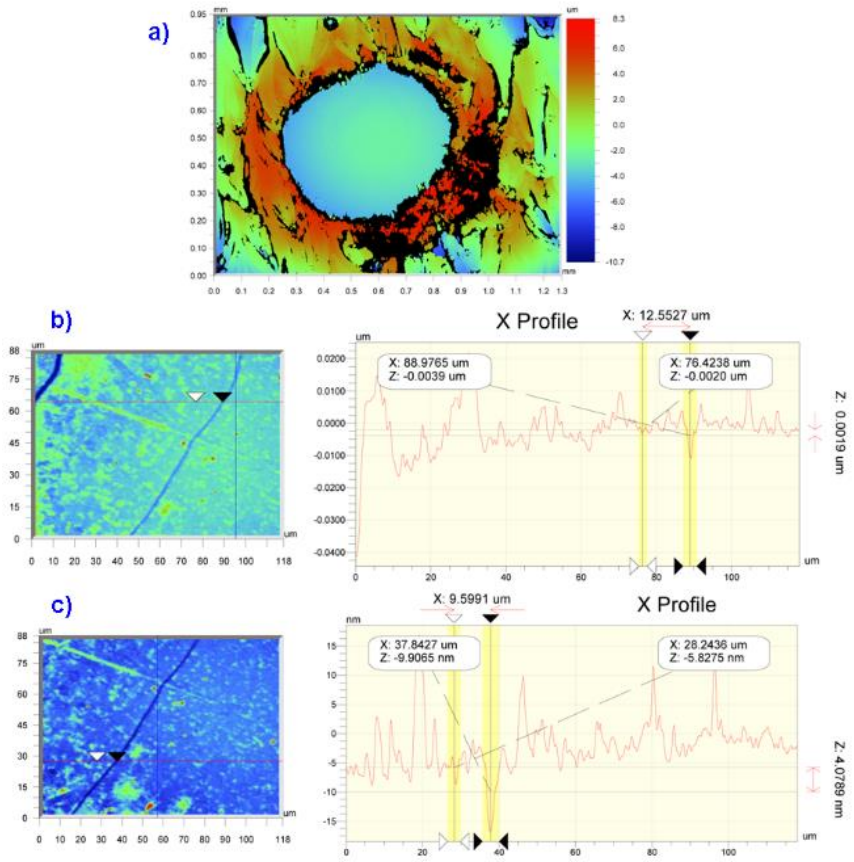

Figure S3. **a)** Optical profilometry image of the d = 600 µm working electrode, **b)** a 2D thickness profile of a crack in the TiO_2 film, revealing the thickness of the film at *ca.* 2 nm, **c)** a 2D line scan thickness profile of another electrode showing a crack height of *ca.* 4 nm.

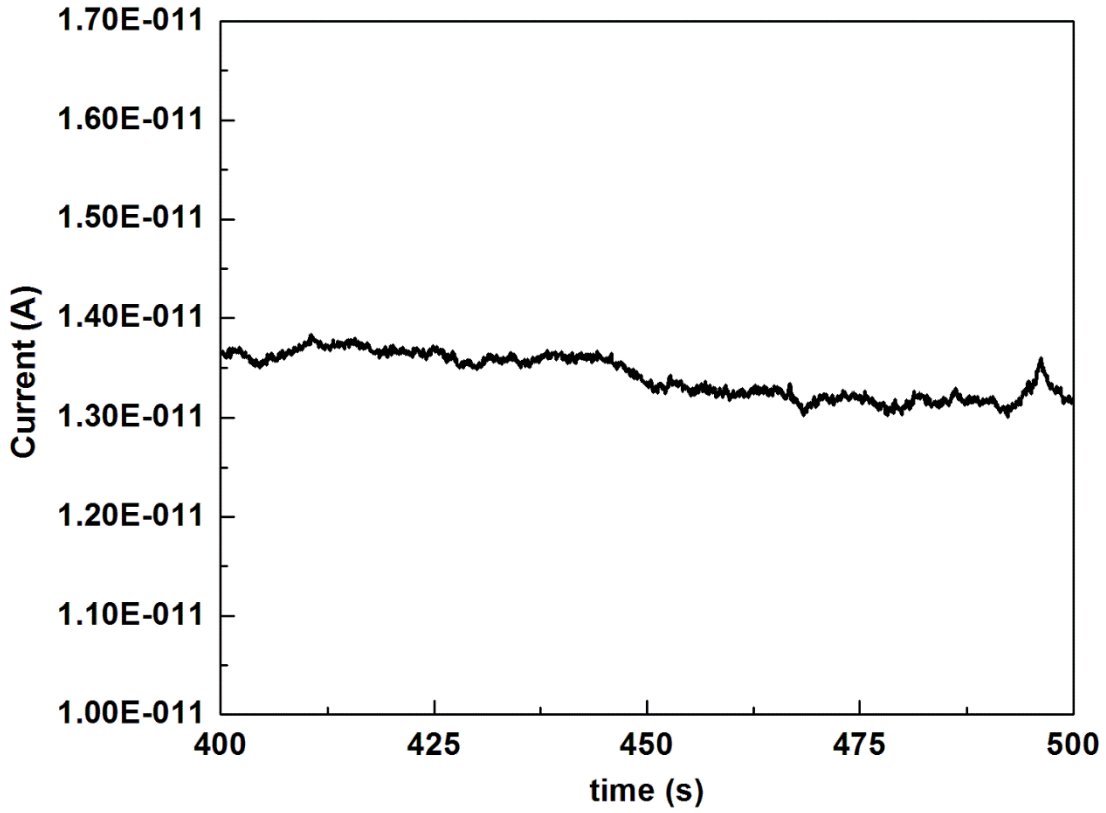

Figure S4. A chronoamperogram obtained from a d = 600 µm electrode of n-Si in the presence of 1 pM Pt NP (7 mM $K_3Fe(CN)_6$, 50 mM phosphate buffer pH 9, and V = -0.4 V vs. Ag/AgCl). The n-Si employed here was cleaned as described above, and then was aged in oxygen saturated water for 72 h for the growth of native SiO_2. No NP collision was observed.

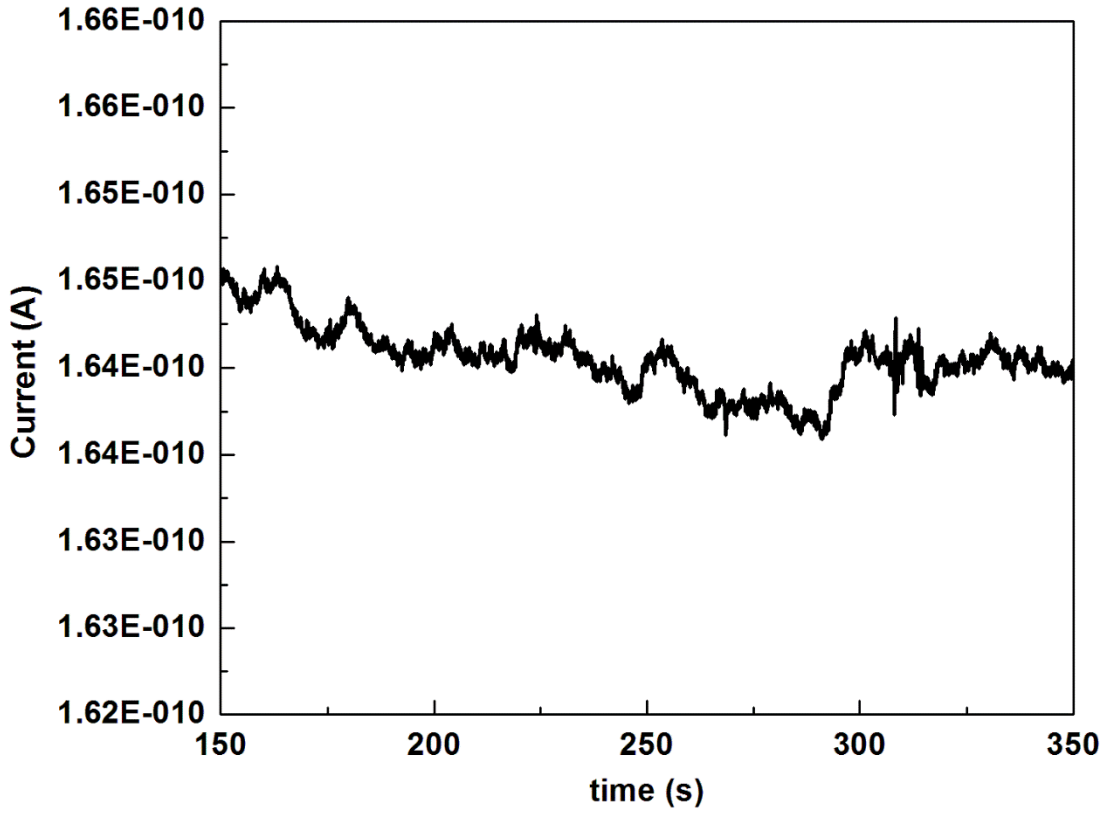

Figure S5. A chronoamperogram obtained from a TiO_2/n-Si electrode in the absence of Pt NP (7 mM $K_3Fe(CN)_6$, 50 mM phosphate buffer pH 9, and V = -0.4 V vs. Ag/AgCl). Noise level of *ca.* 300 fA achieved.

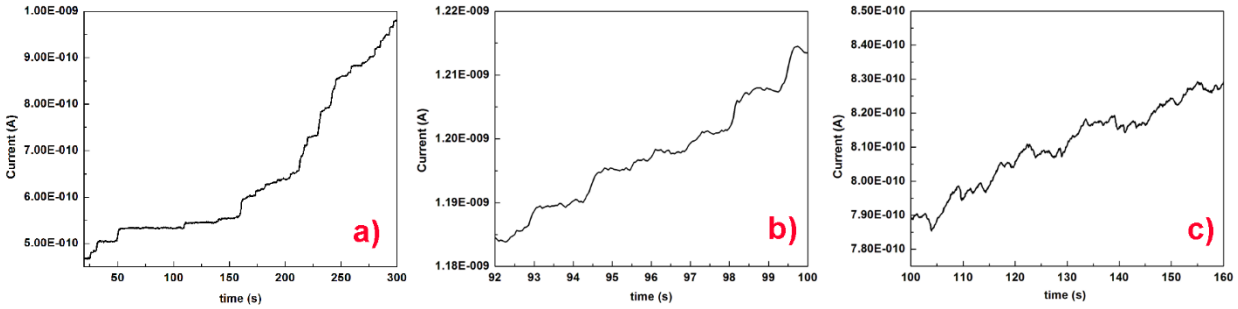

Figure S6. **a)** Chronoamperogram obtained from a TiO_2/n-Si electrode during a NP collision experiment exhibiting many clear step-like collision events. **b)** Chronoamperogram obtained from a TiO_2/n-Si electrode during a NP collision experiment after *ca.* 100 collisions. The current steps become less defined due to the increase in the steady-state background current, and also presumably due to the interaction of the incoming particle with particles on the electrode surface. **c)** Chronoamperogram obtained from a TiO_2/n-Si electrode during a NP collision experiment after *ca.* 300 collisions. The observed current steps become much less defined and the overall current increase becomes small, suggesting that most of the sites available for NP sticking are occupied. In all of the experiments shown above, the solution analyte was 6 mM $K_3Fe(CN)_6$. A 50 mM phosphate buffer solution at pH 9 was employed, and the working electrode was at V = -0.4 V vs. Ag/AgCl.

Table S1. Experimental NP collision frequency compared to that projected from theory using two different NP concentrations obtained from storage solution (2 mM citrate) and experimental solution (50 mM phosphate), respectively. The NP concentration decreased by a factor of 10 when immersed in 50 mM phosphate buffer (See Figure S5). The adjusted frequency was calculated taking into account this drop in concentration. The frequency calculations were performed based on equations 2 and 3 in the manuscript.

NP Concentration (pM)	Collision Frequency (experimental, Hz)	Collision Frequency (calculated, Hz)	Collision Frequency (calc. adjusted, Hz)
1	0.2	4	0.46
2	0.4	8	0.91
5	0.9	20	2.29

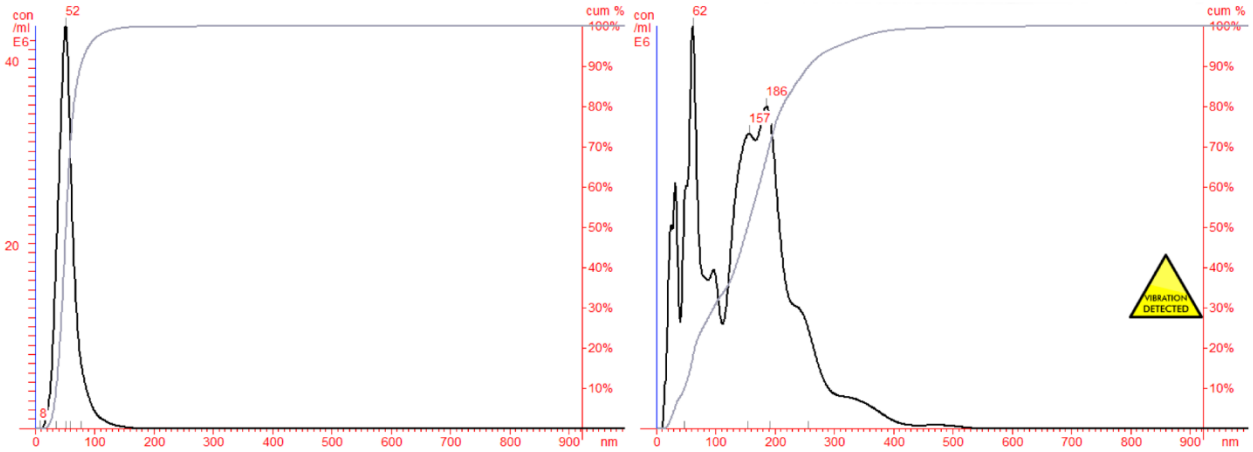

Figure S7. Platinum NP size distribution and concentration obtained from NanoSight NP tracking system – in 2 mM sodium citrate storage solution pH 7.8 (left) when injected into 50 mM phosphate buffer pH 9 (right). Significant aggregation of NPs and decrease in the NP concentration occurred when NPs added to 50 mM phosphate buffered water. The NP concentrations of same dilution were 14 x 10^8 and 1.6 x 10^8 in storage solution (2 mM citrate) and buffered water (50 mM phosphate pH 9), respectively. Concentrations are expressed in number of NPs per mL. Note that the image on the right frame is a snapshot from a stream of NPs, and does not represent the size distribution of the entire batch accurately. The number of 62 nm NPs and that of 157 nm NPs are not equal. The main point illustrated in this figure is the lowered overall concentration of NPs in the buffered solution due to precipitation.

Photocurrent Density Calculation

As seen in Figure 3d in the manuscript, *ca.* 380 pA of photocurrent was obtained from Pt/TiO_2/n-Si electrode with *ca.* 250 Pt NPs on the surface. Simple calculation of the current density based on the geometrical area of the electrode (d = 600 μm) is as follows:

$$(380 \times 10^{-12})\,A \times \frac{1}{(0.03)^2 \times \pi}\ cm^{-2} = 1.34 \times 10^{-7}\ \frac{A}{cm^2} = 0.134\ \frac{\mu A}{cm^2}$$

However, tunneling electron transfer only occurs at n-Si sites that are in contact with Pt NPs, therefore the effective area of the electrode should be defined by the surface area of the 250 Pt NPs. The area may be estimated by treating each NP as independent spheres of radius r = 25 nm. The current density calculated from this effective electrode area is shown below.

$$(380 \times 10^{-12})\,A \times \frac{1}{(25 \times 10^{-7})^2 \times 4\pi \times 250}\ cm^{-2} = 0.0194\ \frac{A}{cm^2} = 19.4\ \frac{mA}{cm^2}$$

It is worth noting that the actual electrode surface area may be higher than that calculated above due to the overlap of diffusion layers of neighboring NPs. However, based on the relative sizes of the electrode and the NP, the actual area is projected to be closer to that used in the above calculation than the geometric area of the d = 600 μm electrode. From the NP size distribution shown in Figure 1d, the estimated upper limit photocurrent density may vary from 10 $mA \cdot cm^{-2}$ (for r = 35 nm NP) to 30 $mA \cdot cm^{-2}$ (for r = 20 nm NP). An NP with r = 25 nm was used for the sample calculation above.

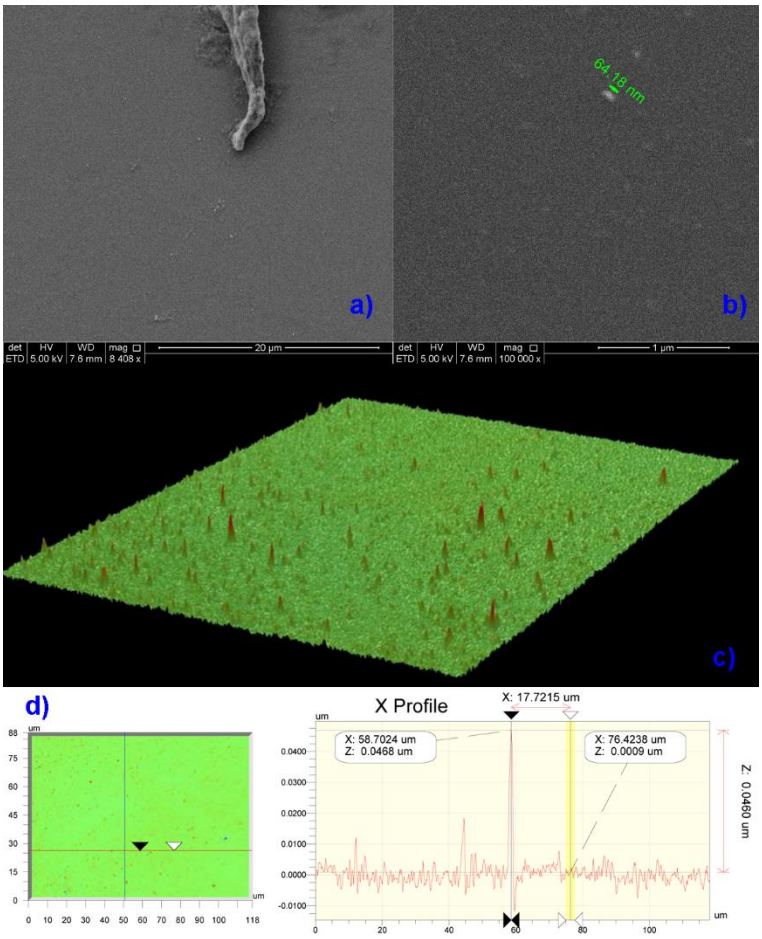

Figure S8. Scanning electron micrographs (SEM) of n-Si surface after a Pt NP collision experiment. **a)** An end of the masking tape can be seen at the top of the image. The surface of the electrode was rather featureless, aside from a few particle aggregates and dust. On the high magnification image in **b)**, a 60 nm NP can be seen, in good agreement with the NP size used in the experiment. Due to the insulating nature of the TiO_2 film, focusing onto such a small object with the SEM was difficult. The image shown in **b)** is characteristic of other regions of the electrode that is a featureless surface with occasional sighting of 50 nm NPs. **c)** A 3D optical profilometry (Wyko profilometer) image of a TiO_2/n-Si electrode with NPs. Each particles shown exhibited good size agreement to those used in the experiment. An example of a NP height is displayed in **d)**, revealing 46 nm. Most NPs were in the 50 nm size range (44 ± 16 nm, 70 particles assessed), similar to the distribution given in Figure 1d.

References

[1] L. Kavan, B. O'Regan, A. Kay, M. Grätzel, *J. Electroanal. Chem.* **1993**, 346, 291.
[2] L. Kavan, T. Stoto, M. J. Grätzel, *J. Phys. Chem.* **1993**, 97, 9493.
[3] M. Morita, T. Ohmi, E. Hasegawa, M. Kawakami, M. Ohwada, *J. Appl. Phys.* **1990**, 68, 1272.
[4] J. Kim, B.-K. Kim, S. K. Cho, A. J. Bard, *J. Am. Chem. Soc.* **2014**, 136, 8173.